

Formation of polyaniline/Pt nanoparticle composite films and their electrocatalytic properties

Anthony P. O'Mullane · Sara E. Dale · Thomas M. Day · Neil R. Wilson · Julie V. Macpherson · Patrick R. Unwin

Received: 14 April 2006 / Accepted: 21 May 2006 / Published online: 8 July 2006
© Springer-Verlag 2006

Abstract Polyaniline (PANI) thin films modified with platinum nanoparticles have been prepared by several methods, characterised and assessed in terms of electrocatalytic properties. These composite materials have been prepared by the in situ reduction of a platinum salt (K_2PtCl_4) by PANI, in a variety of solvents, resulting in the formation of platinum nanoparticles and clusters of different sizes. The further deposition of platinum clusters at spin cast thin films of PANI/Pt composites from a neutral aqueous solution of K_2PtCl_4 has also been demonstrated. Thin-film electrodes prepared from these materials have been investigated for their electrocatalytic activity by studying hydrazine oxidation and dichromate reduction. The properties of the composite materials have been determined using UV–visible spectroscopy, atomic force microscopy and transmission electron microscopy. The nature of the material formed is strongly dependent on the solvent used to dissolve PANI, the method of preparation of the PANI/Pt solution and the composition of the spin cast thin film before subsequent deposition of platinum from the aqueous solution of K_2PtCl_4 .

Keywords Nanoparticle · Conducting polymers · Atomic force microscopy · Electrocatalysis

Introduction

Electronically conducting polymer (ECP)/metal nanoparticle composites have received much attention recently [1–3] due to their potential applications in electrocatalysis [4–14], chemical sensors [15, 16], electrochemical capacitors [17] and protective coatings against corrosion [18]. Various methods for the preparation of these composites have been described, including electrochemical deposition of nanoparticles onto electrodes previously coated with an ECP [5–14], photochemical preparation [19], reduction of metal salts dissolved in a polymer matrix [20, 21], polymerisation of the ECP around nanoparticles [22–24] and mixing of nanoparticles into a polymer matrix [25].

Of the major ECPs, polyaniline (PANI) has proven particularly interesting due to its environmental stability and large conductivity range (over 11 orders of magnitude) [26], controlled to a large extent by the redox state. PANI can exist in four redox states: leucoemeraldine base (reduced form), emeraldine base (EB, half-oxidised form), emeraldine salt (ES, half-oxidised protonated form) and pernigraniline base (fully oxidised form). Only the ES form shows high conductivity, whilst the other forms show low conductivity or essentially act as dielectrics [27]. Numerous examples of the incorporation of metal nanoparticles into PANI have been reported, including Pt [4–14], Au [3, 20, 21, 28–30], Pd [20, 31, 32], Ag [33, 34] and Cu [35, 36]. Of these, PANI/Pt is of interest as it combines the high conductivity of PANI (values as high as 400 S cm^{-1} for a sulphonic acid-doped film [37]) with the excellent catalytic

Dedicated to Professor Dr. Alan Bond on the occasion of his 60th birthday.

A. P. O'Mullane
School of Chemistry, Monash University,
P.O. Box 23, Victoria 3800, Australia

S. E. Dale · T. M. Day · N. R. Wilson · J. V. Macpherson ·
P. R. Unwin (✉)
Department of Chemistry, University of Warwick,
Coventry CV4 7AL, UK
e-mail: P.R.Unwin@warwick.ac.uk

properties of Pt. This type of composite material appears to be extremely promising for the oxidation of small organic molecules [5, 9–14].

Dispersing metal nanoparticles into a conducting polymer matrix can prevent agglomeration of the nanoparticles, resulting in a larger specific area for reaction, whilst maintaining electrical connectivity of the particles to the underlying electrode [3]. Under optimal conditions, this arrangement may result in enhanced electrocatalytic properties compared to the corresponding reactivity of the bulk metal [38, 39]. The PANI/Pt system has been investigated for various electrocatalytic oxidations, including methanol [5, 9–13], formic acid [5, 40], CO [41, 42], hydrogen [6], glycerol [14] and formaldehyde [5]. The hydrogen evolution reaction (HER) [43, 44] and oxygen reduction [45–47] have also received attention.

In this paper, we develop simple methods for forming PANI/Pt composite materials and assess the effect of processing parameters on composite formation. It is well known that the solvent used for dissolving PANI(EB) has a dramatic effect on its conductivity [48]. Strong acids, such as formic acid, convert PANI(EB) into the conducting ES form, whereas solvents like 1-methyl-2-pyrrolidinone (NMP) maintain PANI in the EB form [37], which is poorly conducting. Four methods are investigated in this study for the formation of PANI/Pt composites:

- (A) chemical reduction of a platinum salt (K_2PtCl_4) by PANI dissolved in various solvents, i.e. in situ nanoparticle formation;
- (B) maximising in situ nanoparticle formation;
- (C) solvent role in the chemical reduction of K_2PtCl_4 from aqueous solution at spin-coated PANI films;
- (D) further Pt deposition on PANI/Pt prepared by method A.

These electroless methods contrast with the most popular approaches for producing ECP/Pt nanoparticle composites, involving electropolymerisation of PANI followed by electrodeposition of Pt [5–14]. However, in relation to the work in this study, the electroless deposition of Pd nanoparticles at electro-reduced, acid-doped PANI films has been investigated recently [49].

A particular focus of the paper is on method D, to investigate the role of pre-formed Pt in spin cast films, on further Pt nanoparticle formation from solution. The driving force for Pt nanoparticle formation in all cases is that PANI serves as an electron donor and the platinum salt as an electron acceptor, which results in the oxidation of the PANI and reduction of the platinum salt to metallic platinum.

The electrocatalytic behaviour of the composite films is investigated by hydrazine oxidation and dichromate

reduction. The former involves the following overall reaction:



Hydrazine is of interest from an environmental point of view, as a possibility of realising a zero emission fuel cell [50, 51]. The electroanalytical detection of hydrazine is also of practical importance [52, 53], as hydrazine has been identified as a carcinogen and a hepatotoxin, whose level needs to be controlled in hydrazide drugs.

The reduction of dichromate at noble metal electrodes is regarded as an intriguing example of electrocatalytic behaviour and has been studied by several authors [54, 55]. It is a useful and complementary test reaction to probe the electrocatalytic properties of the PANI/Pt composites fabricated in this work. The need for conducting polymer sensors that operate in neutral aqueous media is potentially significant for biosensors [15, 16], and a further outcome of the work in this study is that the PANI/Pt composites produced are redox active at neutral pH. The work reported in this study represents a full account of limited preliminary data published by us earlier as a communication [56].

Experimental

Materials and chemicals

All chemicals were used as received and were PANI(EB) (Panipol), dimethyl sulfoxide (DMSO) (analytical grade, Fisher Chemicals), formic acid (ACROS Organics), 1-methyl-2-pyrrolidinone (Aldrich), H_2SO_4 (98%, Aldrich), potassium sulphate (AnalR), potassium dichromate (Aldrich), hydrazine (ACROS Organics), high-purity acetone (Fisher Chemicals) and propan-2-ol (HPLC grade, Fisher Chemicals). All aqueous solutions were prepared from Milli-Q reagent water (Millipore). Platinum wire (Goodfellow, 99.99 % purity) was treated before use by polishing with fine-grade emery paper followed by washing with Milli-Q reagent water.

Procedures

Glass, quartz and indium tin oxide (ITO) substrates were cleaned by sonicating for 10 min in acetone, then in propan-2-ol, and were finally blown dry with nitrogen.

Thin-film formation

PANI(EB) films For films cast from DMSO, 0.1 wt% of PANI(EB) was used, and spin coating was achieved at 2,500 rpm for 60 s. Films cast from formic acid utilised

1 wt% of PANI(EB), and spin coating was realised at 2,000 rpm for 60 s with a 1-s ramp time. For films cast from NMP, 0.5 wt% PANI(EB) was used, and substrates were spin-coated at 3,500 rpm. Each PANI(EB) solution was made by sonicating the PANI(EB) powder in the appropriate solvent for 1 h, which was then filtered through a 0.2- μm tetrafluoroethylene (PTFE) filter. The spin coating conditions cited were the optimum found for each

system; the variation arises from the different solubilities of the polymer in each solution and the characteristic evaporation rate of each solvent during the spin coating procedure.

PANI/Pt films Using DMSO as the solvent, varying concentrations of K_2PtCl_4 , dissolved in DMSO, were added to a PANI(EB) solution so that the final concentration of PANI(EB) was 0.1 wt%. Using formic acid as the solvent,

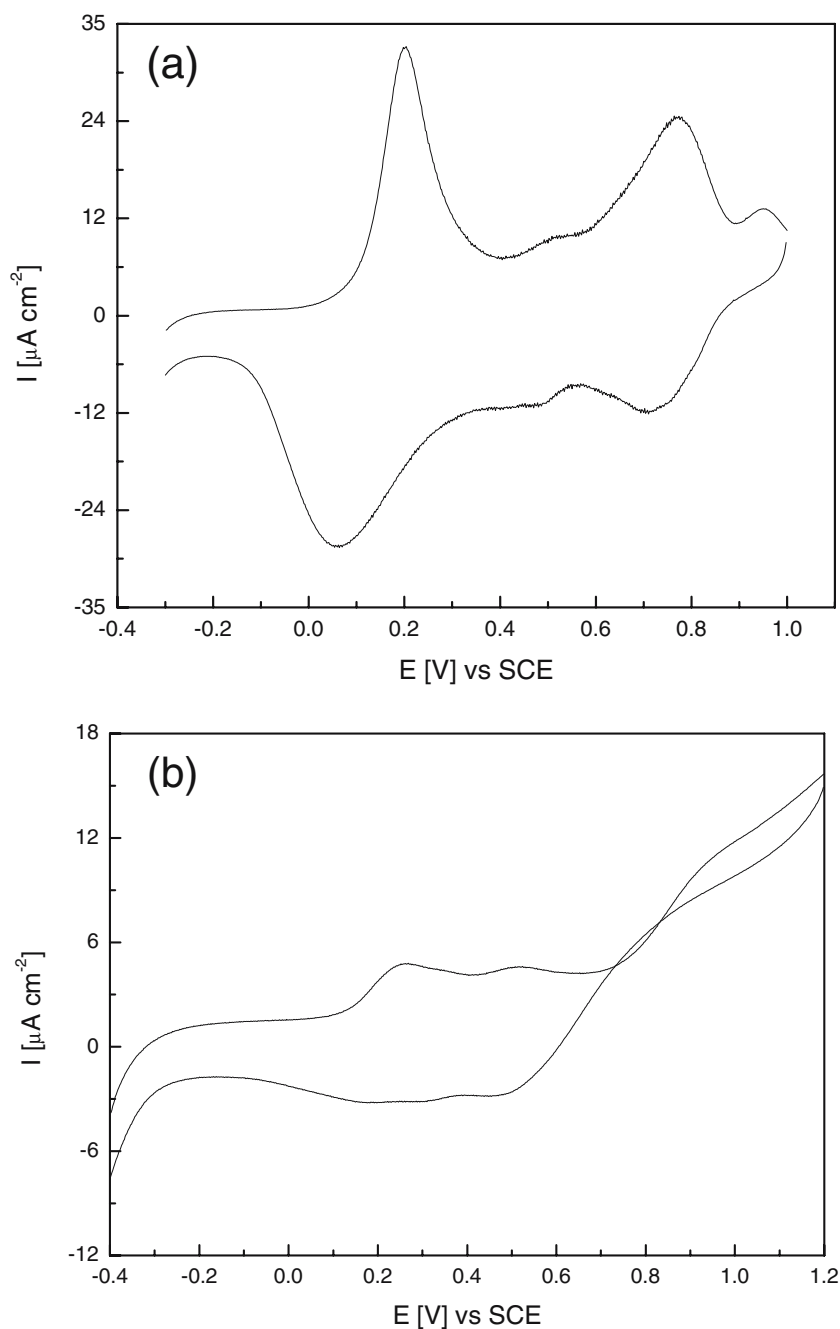


Fig. 1 Cyclic voltammogram of **a** PANI (0.1 wt% in DMSO) film in 1 M H_2SO_4 and **b** PANI/Pt (0.1 wt% in DMSO/5 mM K_2PtCl_4) film in 1 M H_2SO_4 and 0.1 M N_2H_4

K_2PtCl_4 was made up to a concentration of 10 mM in formic and added to a solution of PANI(EB) so that the final concentration of PANI(EB) was 1 wt%. When NMP was employed as the solvent, K_2PtCl_4 was made up to a concentration of 5 mM in NMP and added to a solution of PANI(EB) so that the final concentration of PANI(EB) was 0.5 wt%. In all of the cases described, the solutions were sonicated for 1 h and filtered through a 0.2- μ m PTFE filter.

Cyclic voltammetry (CV) All measurements were made in a three-electrode arrangement using an electrochemical analyser (CH Instruments, model CHI 400). An ITO-covered glass substrate was used as the working electrode (area = 0.85 cm²), a large area platinum gauze served as the counter electrode and a saturated calomel electrode (SCE) was used as the reference electrode. Before each CV measurement, the PANI/Pt films were immersed in water for 30 min to allow any residual K_2PtCl_4 to leach out. All solutions were purged with oxygen-free nitrogen before use. All CV experiments carried out for the investigation of PANI or PANI/Pt were as spin cast films on ITO and were recorded at 50 mV s⁻¹.

Sample irradiation Samples were illuminated for 30 min with a visible-ultraviolet light source (150 W, XBO short arc Xenon lamp, Olympus, Tokyo, Japan) at a working distance of 15 cm.

Transmission electron microscopy (TEM) sample preparation TEM samples were prepared by dipping the TEM grid into a dilute solution of PANI (0.05 wt% in NMP or 0.1 wt% in formic acid) or a PANI/Pt solution (0.05 wt% NMP and 0.5 mM K_2PtCl_6 or 0.1 wt% formic acid and 1 mM K_2PtCl_4), which had been sonicated for 1 h, filtered through a 0.2- μ m PTFE filter, and allowed to dry. To investigate the effect of further Pt deposition, the TEM grid was then immersed in a 10-mM platinum salt solution for 10 s. Finally, the TEM sample was immersed in water for 30 min to remove residual K_2PtCl_4 .

UV-visible spectroscopy All samples were prepared by spin coating onto a quartz substrate, and spectra were recorded with a Perkin–Elmer spectrometer (Lambda 25 UV/Vis spectrometer, Perkin Elmer Instruments, UK).

Atomic force microscopy (AFM) imaging All AFM images were recorded using tapping mode AFM (Digital Instruments, Multimode). Sample thickness was measured by scratching the sample with a scalpel and measuring the resultant profile in contact mode AFM.

Results and discussions

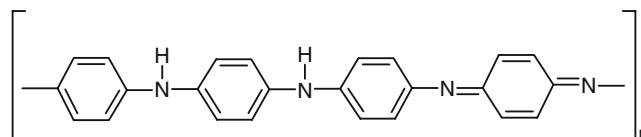
There are many reports in the literature on the electrochemistry of films of PANI/Pt composites [5–14], but these have tended to be for electrodeposited films which have

thicknesses of the order of 0.1 μ m and greater. In this work, we focus on much thinner spin cast films.

In situ nanoparticle formation

Films prepared in dimethyl sulfoxide (DMSO)

UV-visible absorption spectroscopy DMSO was employed as the solvent, as it dissolves K_2PtCl_4 readily but does not protonate PANI(EB). The UV–visible absorption spectrum of a thin film of PANI(EB) showed peaks at 327 and 624 nm due to π – π^* transitions in the aromatic rings of benzene and the benzenoid-to-quinoid exciton transition, respectively [57]. Upon the addition of K_2PtCl_4 , a slight colour change of the solution, from blue to blue-green, was observed by eye which intensified during the sonication procedure. A thin film prepared from such a solution showed a peak at 423 nm and a broad feature with a maximum at 893 nm; features indicative of doped PANI [57]. The surface coverage of PANI was estimated from the UV–visible absorption spectrum and calculated to be $1.2 \pm 0.2 \times 10^{-9}$ mol cm⁻², for the repeat unit illustrated below, with a molar extinction coefficient of 2.2×10^4 M⁻¹ cm⁻¹ ($\lambda=630$ nm) [58].



Cyclic voltammetry CV measurements were carried out on a PANI film in 1 M sulphuric acid. Typical results are shown in Fig. 1a, where well-defined anodic features at 0.20 and 0.78 V on the forward sweep (and corresponding features on the reverse sweep) are observed. These peaks

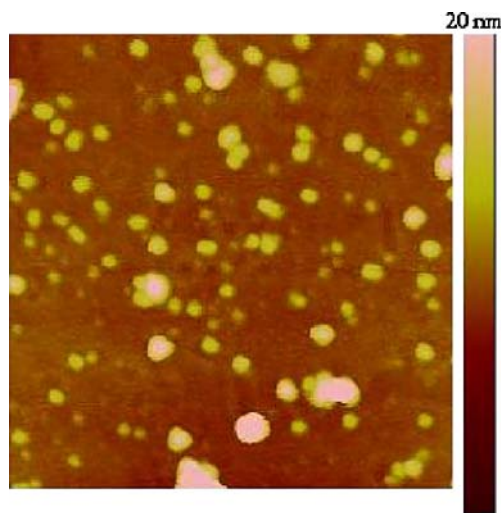


Fig. 2 Tapping mode AFM image (1×1 μ m) of a PANI/Pt (0.1 wt% in DMSO/5 mM K_2PtCl_4) film on glass

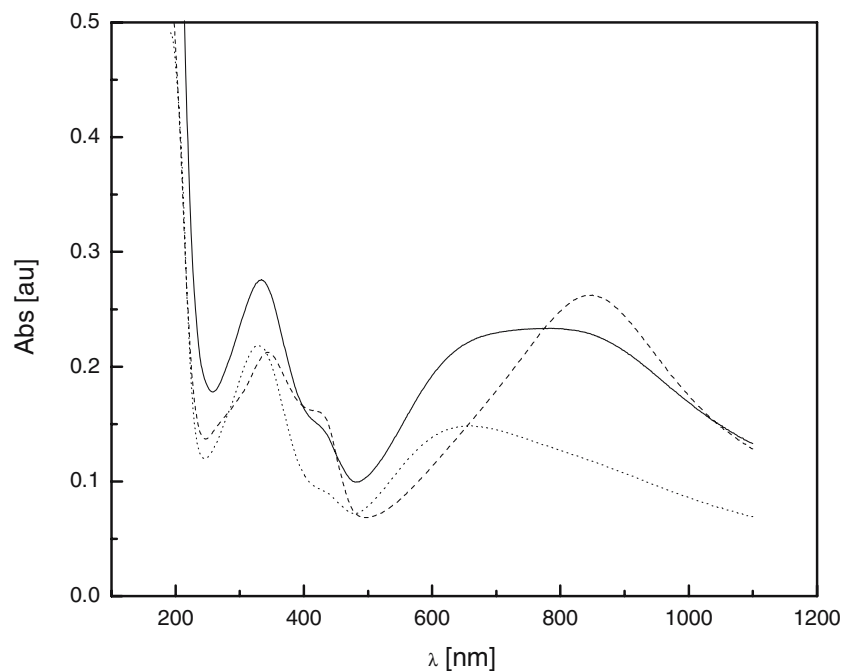


Fig. 3 UV–visible absorption spectra of a PANI film (1 wt% in formic acid) (*dashed line*), an annealed PANI film (*dotted line*) and an annealed PANI/Pt film (1 wt% in formic acid/10 mM K_2PtCl_4) (*solid line*) on quartz substrates

are due to the transition from the leucoemeraldine to emeraldine (EB) oxidation state and from the emeraldine to pernigraniline oxidation state, respectively [52]. The surface coverage of PANI was also estimated from the CV response by integrating the charge passed in the first redox transition (two electron-transfer from the leucoemeraldine state to the EB form, based on the above repeat unit) and found to be $6.2 \pm 0.8 \times 10^{-10}$ mol cm^{-2} . This is in reasonable

agreement with the value quoted above, obtained by UV spectroscopy; the difference between the absorbance and electrochemical results may be due to deviation from the Beer–Lambert Law for ultrathin films, as reported previously for black soap films [59].

CV experiments were then performed on a PANI/Pt electrode in the presence of hydrazine. The latter is electrochemically inactive at ITO and PANI, and any

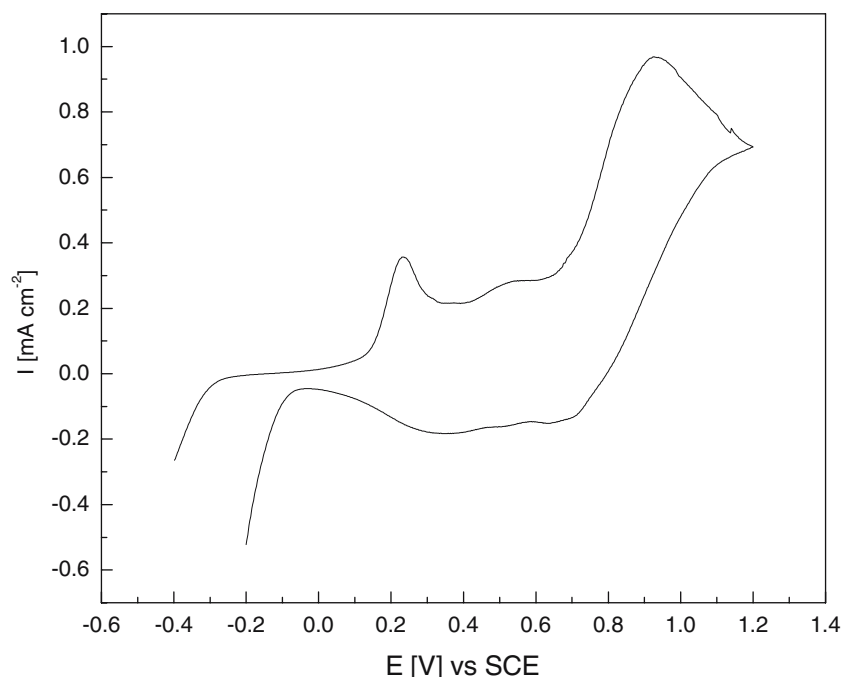


Fig. 4 Cyclic voltammogram of PANI/Pt film (1 wt% in formic acid/10 mM K_2PtCl_4) in 1 M H_2SO_4 and 0.1 M N_2H_4

oxidation current would imply the presence of Pt in the PANI film. Illustrated in Fig. 1b is a typical CV recorded for a PANI/Pt film electrode. It can be seen quite clearly that a small response for hydrazine oxidation was observed. It is also interesting to note that there is an increase in cathodic current as the potential is scanned in the negative direction, which is indicative of the HER. This response again can only be due to the presence of platinum, as the HER occurs neither at PANI nor at ITO at these potentials.

AFM measurements An AFM image of PANI/Pt films spin-cast onto glass substrates are shown in Fig. 2. It can be seen that Pt particles of various sizes have been formed in the range of 5–100 nm diameter. The use of a glass substrate ensured that the driving force for Pt formation was the oxidation of PANI and reduction of the platinum salt.

The PANI films were extremely thin, and the thickness could not be determined precisely with AFM. Based on the CV and UV–visible absorbance measurements, which reveal the surface coverage, we estimate a film thickness in the range of 2–5 nm, assuming a compact film.

Films prepared in formic acid

UV–visible absorption spectroscopy Formic acid dissolves PANI(EB) quite readily and also protonates PANI(EB) to the emeraldine salt form which is conducting, thus allowing the effect of protonated PANI on platinum nanoparticle formation to be investigated. Note that this corresponds to a concentration of 28 mM compared to 2.8 mM used with DMSO as the solvent; this was the maximum concentration achievable in the latter case. The characteristic features of the PANI(ES) form were again observed as a peak at 420 nm and a broad absorption peak centred at 848 nm (dashed line, Fig. 3). This transformation to the ES form could be reversed to a good degree by annealing the composite film on a hot plate (50 °C for 120 s). This drives out residual formic acid present in the film, and the colour of the film changes from green to blue, consistent with the previous work on films cast from formic acid [60].

A spectrum of an annealed film is shown in Fig. 3 (dotted line): the peak at 420 nm was found to decrease considerably, and the broad absorption previously centred at 848 nm shifted to 655 nm, indicating the presence of PANI(EB). This procedure was repeated for PANI/Pt films prepared using 10 mM K_2PtCl_4 . Annealing a spin cast film of this type resulted in a visible colour change from green to blue-green. The spectrum of the annealed film, in Fig. 3 (solid line), indicates that the characteristic features of doped PANI are still present, i.e. there is peak at 420 nm and a broad absorption feature now centred at ca. 780 nm. Even though the residual formic acid has been driven out of the film by annealing, PANI remains in an oxidised form.

The surface coverage of PANI in the formic acid case was determined to be $6.8 \pm 0.4 \times 10^{-9}$ mol cm^{-2} by UV–visible absorption spectroscopy. The latter value was determined for an annealed PANI film (dotted line in Fig. 3) enabling the molar absorption coefficient for PANI(EB) to be used for the surface coverage measurement.

Cyclic voltammetry CV experiments were carried out with PANI/Pt composite films and were also found to be active for both the HER and hydrazine oxidation, as illustrated by the data in Fig. 4. These results prove that Pt formation occurs in the formic acid solution used to prepare the film. The surface coverage of PANI determined by CV (using the method outlined above for the DMSO system) was $5.1 \pm 0.6 \times 10^{-9}$ mol cm^{-2} . The difference between the films produced from the two solvent systems (compare Fig. 4 with Fig. 1b) is the background response for PANI, which is much more prominent for the formic acid system. This is due to the higher surface coverage of PANI on the ITO electrodes in the latter case. The films cast

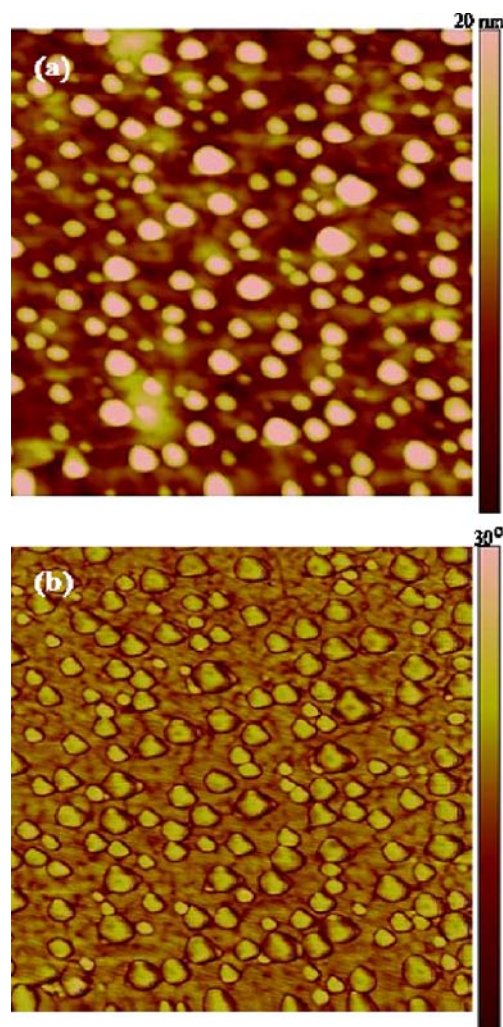


Fig. 5 Tapping mode AFM images ($1 \times 1 \mu m$) of **a** PANI/Pt film (1 wt% in formic acid/10 mM K_2PtCl_4) and **b** corresponding phase image of the same area

from formic acid were found to have a thickness of 25 ± 4 nm, as determined by AFM.

AFM measurements Typical AFM images of PANI/Pt films cast from formic acid are shown in Fig. 5. The morphology shows well-dispersed particles ranging from 30 to 90 nm in diameter, with most particles having a diameter of 50 nm. The corresponding phase image, in Fig. 5b, indicates that these are single particles and not aggregations of smaller particles. Comparing the images in Fig. 5 with that in Fig. 2, it is clear that Pt nanoparticle formation is more extensive when formic acid is the solvent. A major factor is likely to be the initial higher concentration of PANI used. Moreover, in formic acid, PANI is in the conducting ES form, which undergoes oxidation to the pernigraniline form, providing electrons for the reduction of PtCl_4^{2-} to metallic Pt. In acidic media, the pernigraniline form may undergo subsequent reduction to the ES form [49], and so the electroless process may be sustained by a cycle of polymer reprotonation and reduction.

Films prepared in 1-methyl-2-pyrrolidinone (NMP)

UV-visible absorption spectroscopy NMP was considered as a solvent because it dissolves PANI readily but, unlike formic acid, does not protonate PANI. The increased solubility of PANI in this solvent, in comparison to DMSO, allows one to observe more directly the role that the acidic

nature of the solvent plays in in situ Pt formation. However, the solubility of the platinum salt in NMP is quite poor, and the maximum concentration used was limited to 5 mM. A concentration of 0.5 wt% of PANI was chosen to maintain the ratio of PANI to the platinum salt, at the level used for the study with formic acid (1 wt% PANI and 10 mM K_2PtCl_4). It was noticeable that the PANI/Pt composite solution did not change colour (compared to PANI alone) but remained deep blue. The UV–visible absorption spectrum of PANI/Pt films prepared from NMP showed characteristic features of the EB form but not for the ES form. However, previous vibrational spectroscopic studies on PANI(EB) treated with platinum(IV) chlorocomplexes in H_2O revealed that platinum is incorporated into PANI in various oxidation states, which results in the oxidation of PANI [61]. The surface coverage of PANI was calculated to be $1.6 \pm 0.4 \times 10^{-9}$ mol cm^{-2} (by the same procedure as for DMSO), and a film thickness of 6 ± 2 nm was determined by AFM.

Cyclic voltammetry CV experiments performed with PANI/Pt composite electrodes (surface coverage of PANI was calculated to be $1.4 \pm 0.7 \times 10^{-9}$ mol cm^{-2}) showed activity for both the HER and the oxidation of hydrazine. The latter reaction was quite sluggish, but the observation of voltammetric characteristics for both processes indicated that platinum formation occurred in the NMP solution.

AFM measurements AFM images of a PANI/Pt film showed no obvious Pt particle formation in contrast to the

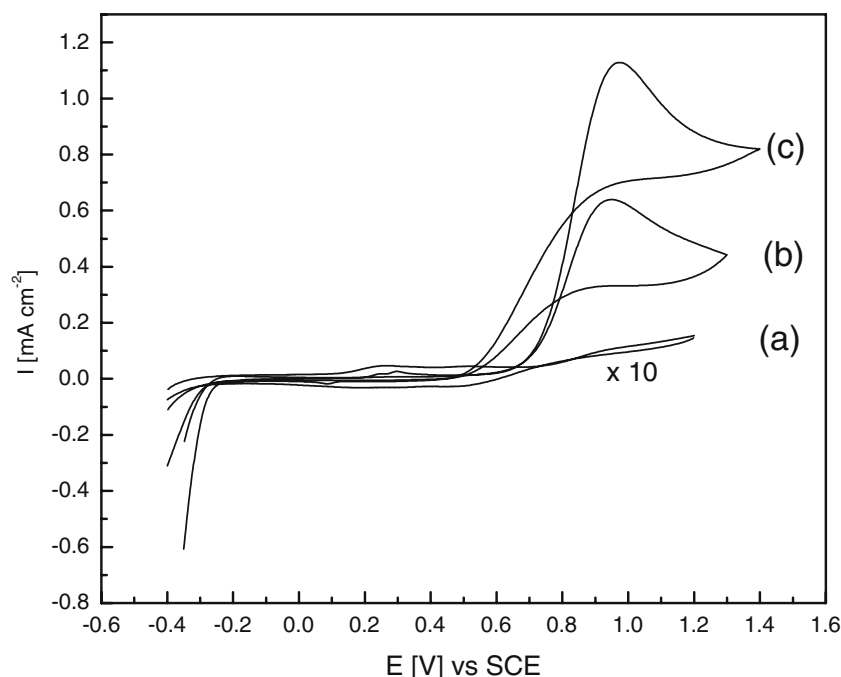


Fig. 6 Cyclic voltammograms of PANI/Pt films prepared from 0.1 wt% PANI in DMSO by **a** in situ formation with 5 mM K_2PtCl_4 (current scale has been multiplied by a factor of 10), **b** irradiation of a film for

30 min fabricated in **(a)** and **c** in situ formation with 20 mM K_2PtCl_4 in 1 M H_2SO_4 and 0.1 M N_2H_4

cases of DMSO and formic acid solvents. This suggests that two factors may be influencing the extent of in situ Pt formation; the aprotic nature of the solvent and the driving force for a redox interaction between PANI(EB) and K_2PtCl_4 . In the NMP case, this interaction is quite limited when compared to DMSO, another aprotic solvent. It should also be noted that the film quality was quite poor in comparison to that observed in the formic acid case, which suggests that some type of separation may be occurring between dissolved PANI and K_2PtCl_4 , which subsequently results in less Pt formation compared to DMSO.

Maximising in situ nanoparticle formation

Two methods were employed to increase the extent of in situ nanoparticle formation in each of the solvents. The first method was to simply increase the concentration of K_2PtCl_4 whilst keeping the PANI concentration constant. The PANI concentration was not varied as the concentrations employed until now were optimised for the best film preparation. The only solvent where an increase in K_2PtCl_4 concentration resulted in further in situ Pt nanoparticle formation was DMSO. Using this method for the other solvents resulted in non-dissolution of the platinum salt or severe precipitation of solid from the solution after a few minutes.

In DMSO, the K_2PtCl_4 concentration was increased to 20 mM, whilst maintaining the PANI(EB) concentration at 0.1 wt%, which corresponds to a concentration of 2.8 mM. These PANI/Pt films showed a tremendous increase in current for the HER and hydrazine oxidation as compared to the composite prepared from the lower platinum salt concentration. This point is highlighted by the data in Fig. 6, which shows the voltammetric responses recorded for hydrazine oxidation for films prepared from 5- and 20-mM K_2PtCl_4 . In the latter case, there was a startling 100-fold increase in hydrazine oxidation current as compared to the use of 5 mM K_2PtCl_4 . It can also be seen that there is a decrease of the onset potential to a less positive value of ca. 0.61 V.

A typical high-resolution AFM image of films prepared with the higher concentration of K_2PtCl_4 is shown in Fig. 7a, where the image was taken of a typical sized cluster from an isolated region. It can be seen that large clusters of Pt have formed, with diameters up to 150 nm across. In comparison to when the lower concentration of Pt salt was used, there appears to be more extensive in situ Pt formation, which takes the form of larger clusters and explains the higher electrocatalytic activity observed for hydrazine oxidation. It is clear from these results that the concentration of K_2PtCl_4 used in the synthesis of the composite films has a large effect on the resultant formation

of metallic platinum in the spin cast films. To further investigate this, the concentration of K_2PtCl_4 used to prepare the composites was increased to 50 mM, but this

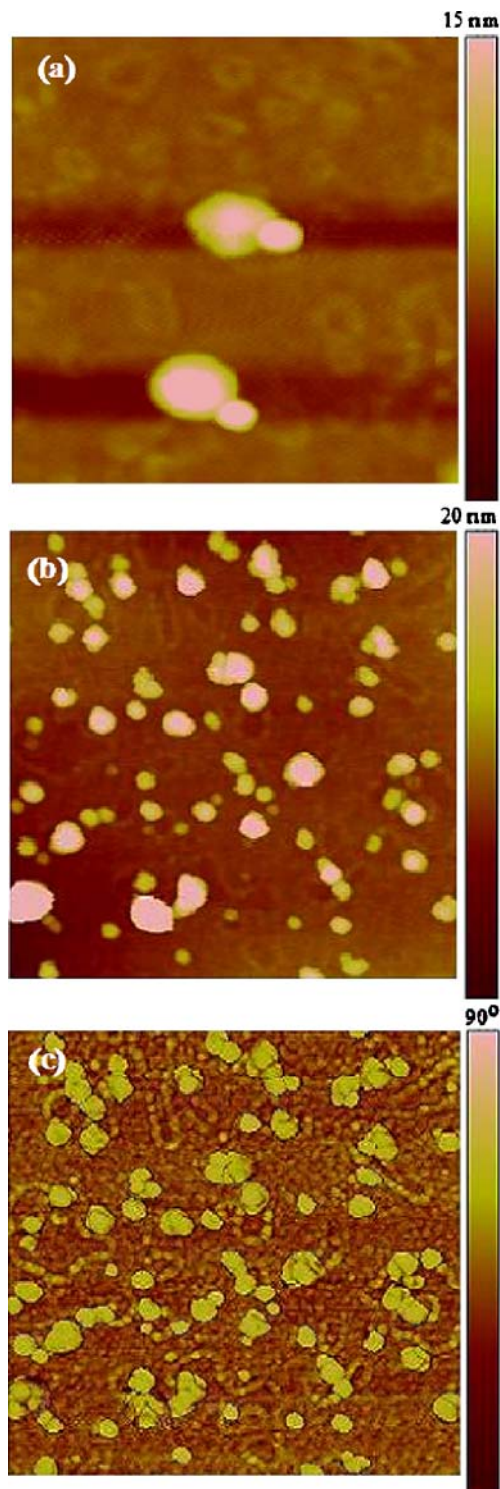


Fig. 7 Tapping mode AFM images of **a** (500×500 nm) of a PANI/Pt film (0.1 wt% in DMSO/20 mM K_2PtCl_4), **b** (1×1 μm) PANI/Pt film (0.1 wt% in DMSO/5 mM K_2PtCl_4) irradiated for 30 min and **(c)** corresponding phase image of the same area in **(b)** on glass substrates

resulted in severe precipitation of material from solution after 1 h.

The second method used to increase in situ formation of Pt was an irradiation procedure. This method has been investigated previously for the photo-reduction of platinum salts present in mesoporous material leading to the formation of metal nanorods, but under quite forcing conditions [62, 63]. Irradiation of a PANI/Pt composite prepared from 0.5 wt% NMP and 5 mM K_2PtCl_4 resulted in a 50-fold increase in performance for hydrazine oxidation in comparison to the non-irradiated PANI/Pt film as seen in Fig. 6. AFM images of particles on the irradiated film in comparison to a non-irradiated film (compare Fig. 7b with Fig. 2) appear to be slightly larger with again a range of sizes. The corresponding phase image for Fig. 7b, shown in Fig. 7c, indicates that the prominent features are not single particles but rather clusters of particles. The corresponding phase image for Fig. 2 is not shown in this paper, as the particles do not consist of smaller individual particles as seen in Fig. 7b. Clusters of smaller particles have greater activity than a single large particle; thus, the dramatic increase in electrocatalytic activity of the irradiated film may be due to a greater surface of platinum being available for reaction.

This irradiation procedure was repeated for a PANI/Pt film prepared with a higher concentration of K_2PtCl_4 (20 mM); however, no increase in hydrazine oxidation current was observed. The irradiation procedure was then employed for PANI/Pt films prepared using formic acid and NMP, but again, no increase in performance was observed. This suggests that for the latter solvents where an excess

concentration of PANI over K_2PtCl_4 was employed, the reaction goes to completion in the dark.

Given the excess concentration of PANI over K_2PtCl_4 , a different approach was needed to maximise the quantity of platinum in these composites. This involved immersing PANI films in an aqueous solution of 10 mM K_2PtCl_4 for 30 min. Under these conditions, there is an unlimited supply of K_2PtCl_4 for the PANI film to react with. This type of approach has been investigated previously for the PANI/Au system, in which electrochemically polymerised PANI films were immersed in an acidic $KAuBr_4$ solution, resulting in spontaneous gold deposition [30], with 400-nm-size clusters formed for immersion times of 30 min.

Chemical reduction of K_2PtCl_4 at spin cast PANI films (method A)

Films prepared from formic acid

This method yielded electrodes with a high activity for the HER, and for hydrazine oxidation in particular, as evidenced by the data in Fig. 8 (dotted line). Compared to the results presented earlier for in situ formation of platinum (Fig. 4), it is interesting to note that the onset potential for hydrazine oxidation for films prepared by this method has shifted dramatically to less positive values, and the current density has increased significantly. This result suggests that this approach results in greater Pt formation than the in situ method. For comparison, Fig. 8 also shows the response recorded at a Pt wire electrode (dashed line) in

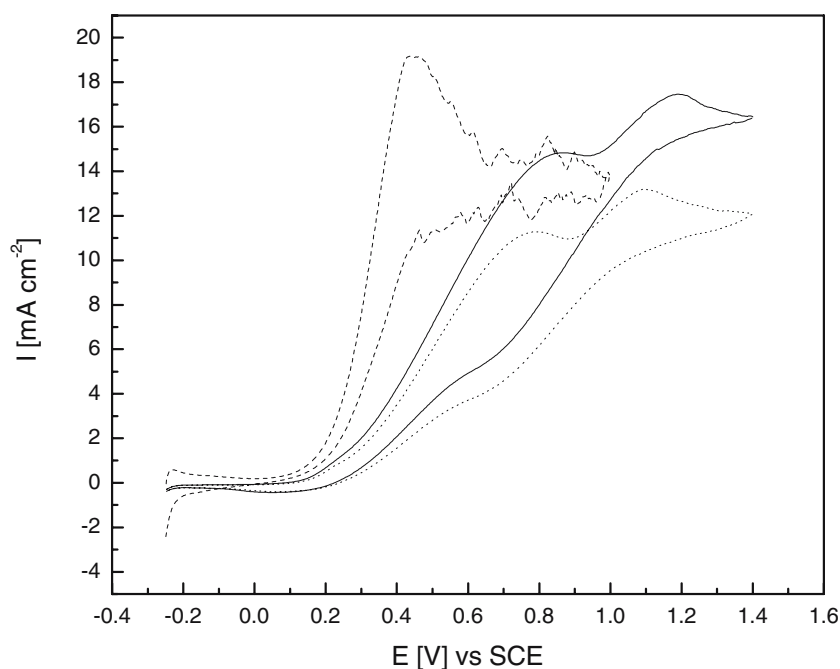


Fig. 8 Cyclic voltammograms of PANI/Pt films (1 wt% in formic acid/10 mM K_2PtCl_4) in 1 M H_2SO_4 and 0.1 M N_2H_4 prepared by method A (dotted line) and Method B (solid line). The response of a Pt wire electrode is shown as the dashed line

the same solution. Moreover, the current densities at the two electrodes (calculated for the overall geometric area) are quite similar, which is noteworthy given the relatively small amount of Pt in the film electrodes.

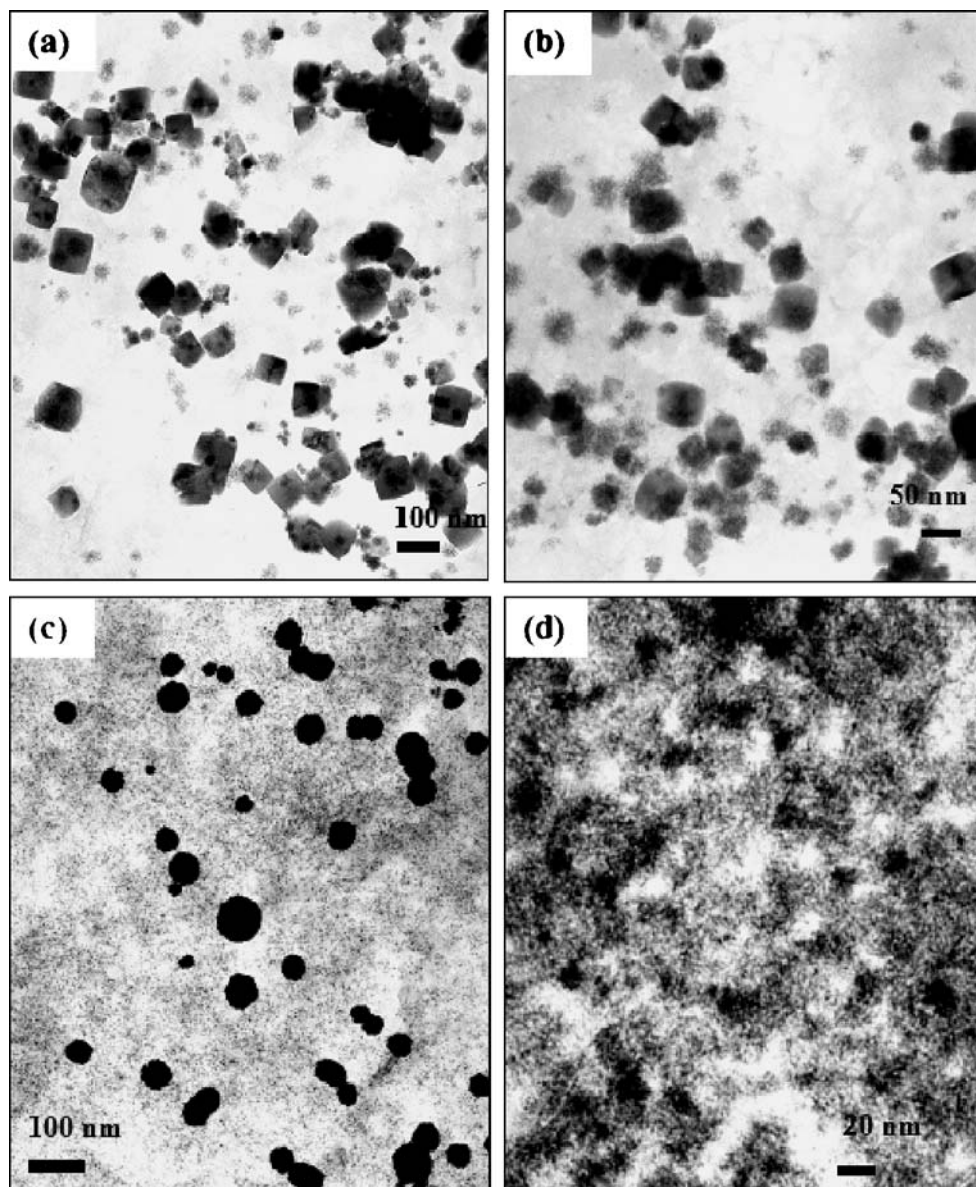
TEM images were taken of films prepared by a slightly modified version of method A. As outlined in the “*Experimental*” section, a lower concentration of PANI solutions was used to ensure that a sufficiently thin film was formed, after the dipping procedure, to allow successful subsequent TEM analysis. The TEM images in Fig. 9a,b of a film prepared by this method show large cubic single crystals of Pt with lengths between 20 and 100 nm. Metallic platinum appears to form at particular sites on the PANI film, and this leads directly to relatively large crystal formation. This differs to the in situ formation where spherical particles were observed.

Films prepared from NMP

For the in situ formation method, UV–visible spectroscopy did not show any indication of PANI oxidation. Using method A, evidence for PANI oxidation to the ES form was observed by the appearance of a broad absorbance centred at 870 nm and a blue shift of 61 nm in the peak centred at 620 nm which is indicative of doped PANI. This blue shift, which has been attributed to an increase in the oxidation state of PANI, has also been reported for the PANI/Au system, where Au nanoparticles were formed in NMP solutions of PANI [20]. Therefore, for PANI in NMP, a large excess of Pt salt is required to measurably increase the oxidation state of PANI.

This method also yielded electrodes with a high activity for the HER and for hydrazine oxidation in particular as

Fig. 9 TEM images of: **a, b** PANI film (0.1 wt% in formic acid) formed by method A; **c, d** PANI/Pt film (0.1 wt% in formic acid/1 mM K_2PtCl_4) formed by method B, both after immersion in 10 mM K_2PtCl_4 for 10 s



evidenced by the data in Fig. 10. However, in comparison to the previous case where formic acid was used as the solvent, the onset potential is much more positive for hydrazine oxidation (ca. 0.61 V vs ca. 0.18 V).

TEM images of films prepared by method A are shown in Fig. 11a,b. These images show that there are platinum deposits, comprising clusters of smaller particles. The clusters are of the order of 30–50 nm across and differ greatly to that observed for the formic acid case where larger cubic crystals were formed. The extent of platinum formation also seems to be less in comparison to the formic acid case and explains the lower current density for hydrazine oxidation.

Further Pt deposition on PANI/Pt composites (method B)

In this method, the same dipping procedure as method A was applied to the original films prepared from PANI/Pt solutions to observe the influence of pre-formed Pt on the deposition step from solution.

Films prepared from formic acid

PANI/Pt electrodes fabricated by method B showed an enhanced performance for hydrazine oxidation compared to method A (Fig. 8). The onset potential has shifted to slightly less positive potentials and is now comparable to that for Pt wire. The similar current densities suggest the formation of a well-packed film of Pt nanoparticles over the entire electrode with this fabrication method. TEM images

of such a PANI/Pt composite shown in Fig. 9c,d support this view. In contrast to the large cubic crystals formed by method A, this procedure results in the formation of particles of the order of 1–2 nm diameter over the entire region of the film, with larger clusters up to 50 nm diameter also evident. It is noteworthy that these clusters, themselves, comprise of 1–2 nm diameter particles. Figure 9d provides a more detailed image of a region without the large clusters, and this indicates that there is a high coverage of 1 to 2-nm-size Pt nanoparticles.

Films prepared from NMP

As found for the composites produced in formic acid, method B shows an enhanced performance for hydrazine oxidation over method A (Fig. 10), which is related to slightly more extensive Pt nanoparticle formation for the latter method as seen in the TEM images shown in Fig. 11c,d. Note, however, that for method B with NMP, the coverage is neither as uniform nor as extensive as when formic acid was used as the solvent. In particular, the 1 to 2-nm-size particles which were observed for the formic acid case over the entire film are significantly absent. This difference again can be explained, as for the in situ formation method, by the difference in the acidic nature of the solvents. The electroless process is not sustained by a cycle of polymer reprotonation and reduction, as suggested for the formic acid case, in aprotic solvents such as NMP. This also explains the difference in the hydrazine oxidation currents at composites prepared in the two solvent systems, with the formic acid

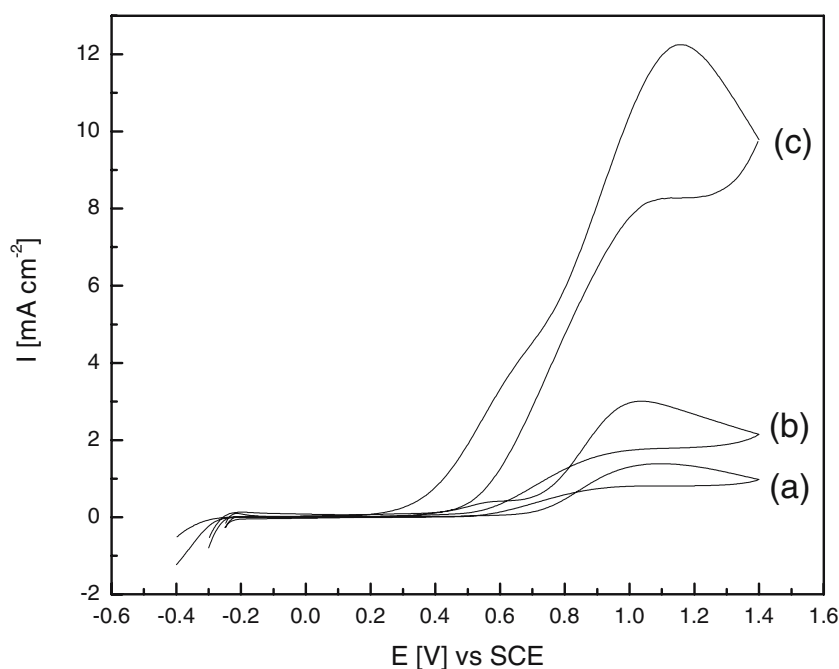
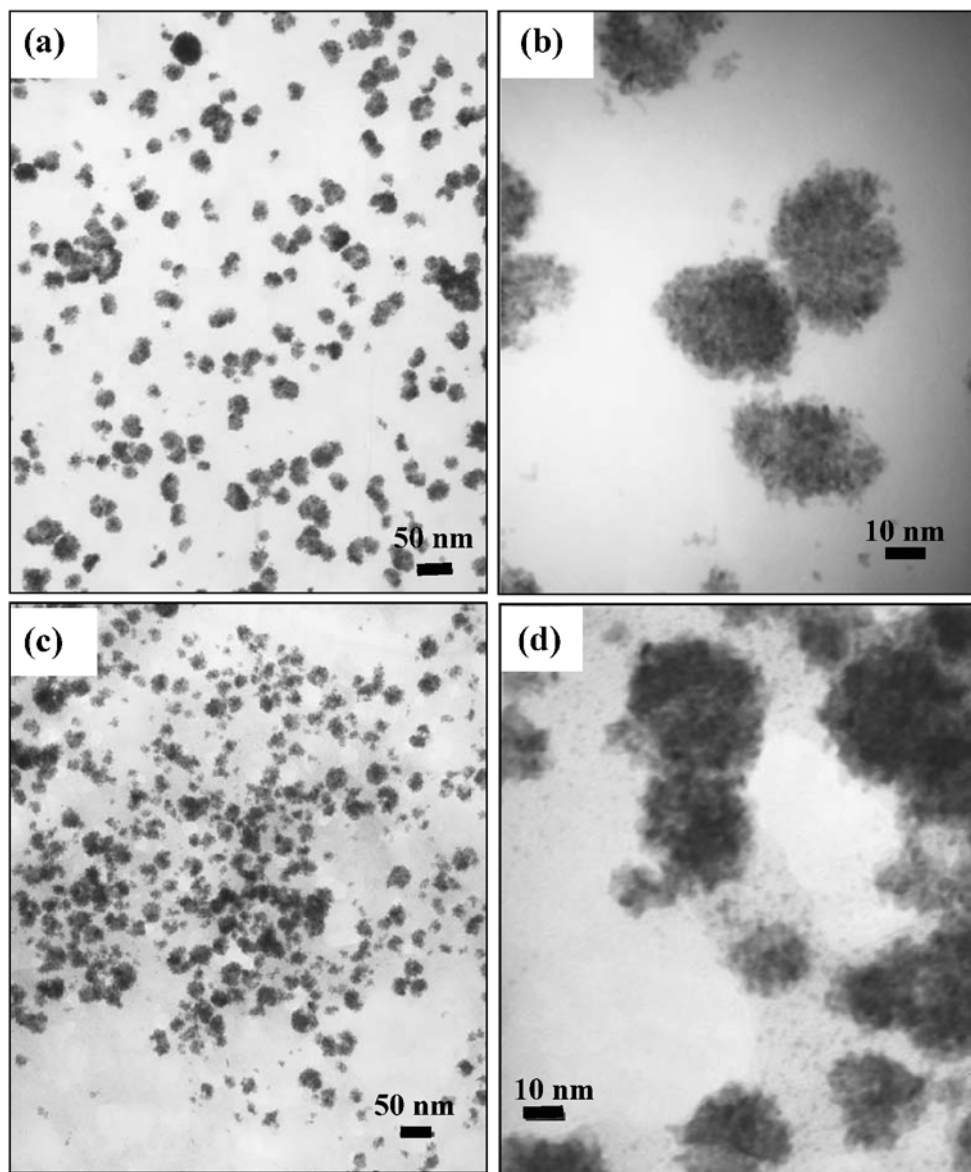


Fig. 10 Cyclic voltammograms of PANI/Pt films (0.5 wt% in NMP/5 mM K_2PtCl_4) in 1 M H_2SO_4 and 0.1 M N_2H_4 prepared by **a** method A, **b** method B and **c** method C

Fig. 11 TEM images of: **a, b** PANI film (0.05 wt% in NMP) formed by method A; **c, d** PANI/Pt film (0.05 wt%/0.5 mM K_2PtCl_4 in NMP) formed by method B, both after immersion in 10 mM K_2PtCl_4 for 10 s



system yielding a current density ca. five times higher than for the NMP system at 1.0 V (SCE).

Addition of LiCl It has been reported that hydrogen bonding between amine and imine sites in PANI(EB), in polar aprotic solvents such as NMP, results in aggregation in the film [64], which may impair film quality and particularly the conductivity. Addition of LiCl to solutions of PANI(EM) in NMP dopes the polymer and interrupts the interchain hydrogen bonding, thus decreasing the extent of aggregation and resulting in improved conductivity [65]. In light of this previous work, a slight alteration to method B was thus investigated. Initially, a film was spin-cast from a solution of 0.5 wt% PANI(EB), 5 mM K_2PtCl_4 and 0.5 wt% LiCl. This was then immersed in an aqueous solution of 10 mM K_2PtCl_4 (method C). Typical CV data for the oxidation of hydrazine at a film formed in this way are

shown in Fig. 10. There was a significant increase in current density at 1.0 V, which was comparable to that obtained when formic acid was used to form the composite. However, the onset potential for hydrazine oxidation was still slightly more positive than for the formic acid system but more favourable than for films formed by method B with NMP. TEM images of a film prepared by method C are shown in Fig. 12. Clusters of the order of 10 nm, made up of small particles of 1 to 2-nm sizes (Fig. 12b), are seen to be evenly distributed over the sample. This is in contrast to method B (Fig. 11c) where large aggregated clusters of particles were observed.

The introduction of LiCl has a dramatic effect on the electrocatalytic performance of these electrodes. This appears to be due to an improved distribution of smaller Pt clusters and an increase in conductivity of the film by the

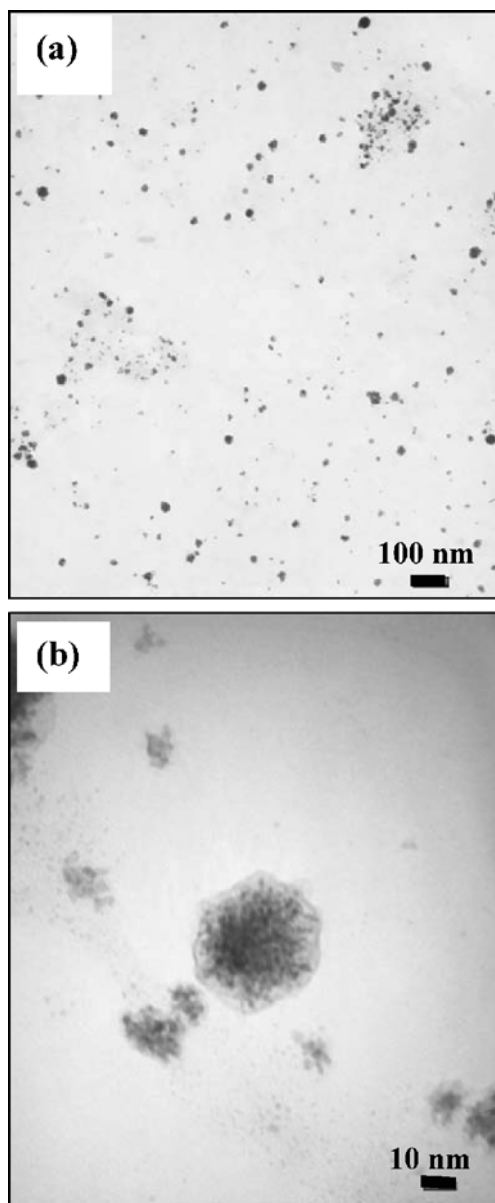


Fig. 12 TEM images of a PANI/Pt film (0.05 wt% in NMP/0.5 mM K_2PtCl_4 /0.5 wt% LiCl), after immersion in 10 mM K_2PtCl_4 for 10 s

addition of LiCl. To determine whether the conductivity of the film plays a role in the formation of platinum nanoparticles, method C was employed, but with the deposition step taking place in an acidic solution of K_2PtCl_4 (to dope the PANI). Electrodes fabricated in this manner did not show any improvement in electrocatalytic activity for the HER or hydrazine oxidation. This suggests that the presence of LiCl dopes PANI(EB) in NMP to its maximum capability, and further treatment in acid has no beneficial effect. This also suggests that Pt nanoparticle formation from solution is more facile at a PANI film prepared from PANI(EB) dissolved initially in formic acid than a

subsequently acidified PANI(EB) film fabricated from PANI(EB) dissolved in NMP.

Dichromate reduction

The electrocatalytic performance of electrodes fabricated by the three different methods, with NMP solvent, was investigated further by examining dichromate reduction. This is a well-known reaction which has been the subject of several studies at bulk noble metal electrodes [54, 55]. Figure 13 shows typical responses, for dichromate reduction (2 mM) in 1 M H_2SO_4 , at PANI, PANI/Pt composite (prepared by method B) electrodes and a platinum wire electrode. It should be noted that a bare ITO electrode showed no activity for this reaction. PANI showed some activity for dichromate reduction, but large enhancement was observed for the PANI/Pt composite electrode. PANI/Pt electrodes prepared by methods A and C showed similar voltammetric behaviour to that illustrated in Fig. 13 for method B. The response for the PANI/Pt electrode is comparable to that of bulk platinum at low potentials (the current densities were calculated using the overall geometric surface area of the electrodes). The significant difference between PANI/Pt and Pt is that an extensive reduction current plateau is observed over a potential range of -0.2 to 0.4 V for the composite electrode, whereas the wire electrode shows a sharp decrease in current at ca. 0 V. The enhanced electrocatalytic current at the composite electrode over a large potential window illustrates the effectiveness of dispersed platinum particles in a PANI matrix for this particular reaction.

Determination of Pt surface area in PANI/Pt films

A standard method to determine the real surface area of platinum in PANI/Pt composite electrodes is to measure the charge passed in the hydrogen adsorption/desorption region [6, 12]. However, for PANI/Pt electrodes prepared by each of the methods outlined and for each solvent, no observable hydrogen region was recorded in 1 M H_2SO_4 solution. Previous studies that have encountered this problem utilised CO stripping experiments [6, 12], where the charge passed in the stripping peak allows determination of the surface area of platinum present in the composite. However, when this method was applied to the PANI/Pt films (for all methods of preparation), no CO stripping peak was detected in a CO-saturated 1 M H_2SO_4 solution. For the formic acid case, strong adsorption of HCOOH could inhibit CO adsorption but this is not the case for the other solvents used in this study. Therefore, the lack of a stripping response may be a consequence of a low concentration of platinum formed by this technique, which we estimate as having a maximum value of $1.3 \mu g cm^{-2}$,

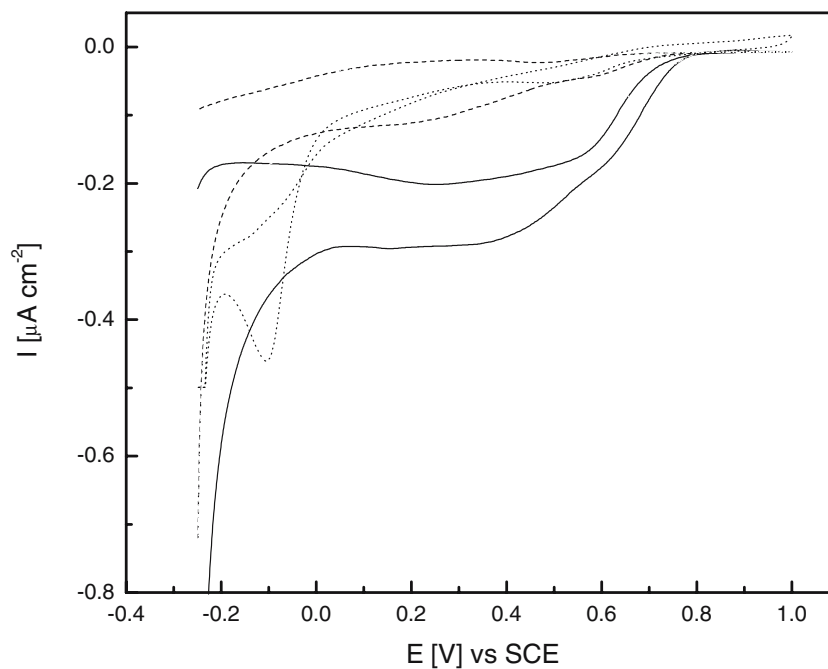


Fig. 13 Cyclic voltammograms of spin cast PANI and PANI/Pt films on ITO substrates, and a Pt wire electrode, in 1 M H_2SO_4 and 0.002 M $\text{K}_2\text{Cr}_2\text{O}_7$ recorded at 2 mV s^{-1} : PANI (—); PANI/Pt prepared by method B (---); and a Pt wire (⋯)

calculated using a surface coverage of PANI of $6.8 \times 10^{-9} \text{ mol cm}^{-2}$ (for the case of formic acid as this composite comprised the highest concentration of PANI), as determined by UV–visible absorption spectroscopy.

Studies at neutral pH

As the formic acid system proved to be optimal for producing electrocatalytically active composite electrodes

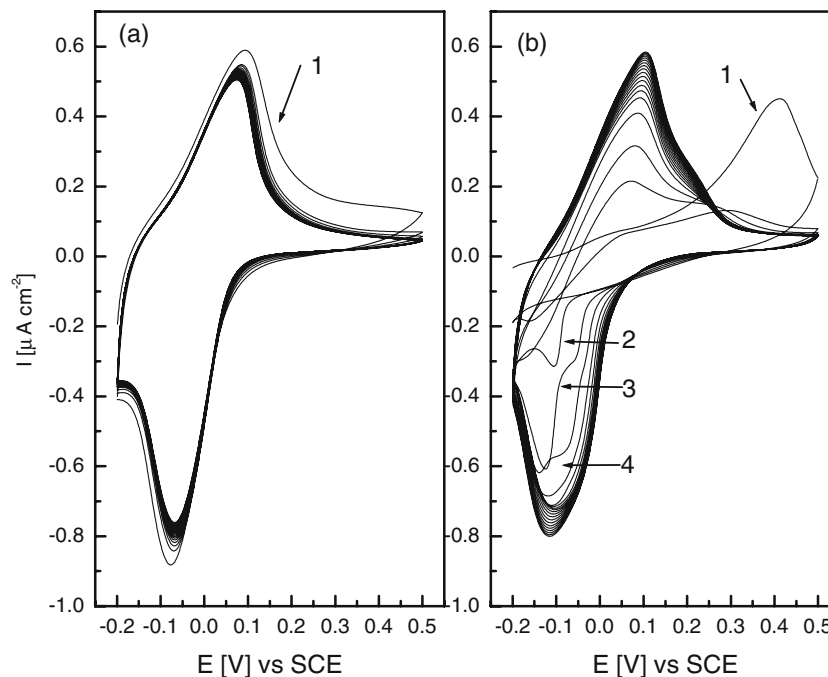


Fig. 14 Cyclic voltammograms (20 cycles) of annealed **a** PANI/Pt film prepared by method B and **b** PANI film, using formic acid as the solvent, in 0.1 M phosphate buffer (pH=7.3). The numbers indicate the cycle

(based on the hydrazine studies), the characteristics of the electrodes in neutral pH aqueous media were explored further. In a 0.1-M phosphate buffer, pH=7.3, the PANI/Pt composite remained active for hydrazine oxidation with a current density of 4 mA cm^{-2} at 0.4 V (SCE), even when the electrode had been annealed on a hot plate (temperature 50 °C for 120 s) to remove any residual formic that would dope the PANI. This is a surprising result as PANI is appreciably conducting only at pH<4. To understand the redox characteristics of the PANI/Pt composite, we compared its activity to a PANI electrode. The PANI/Pt electrode was immediately redox active, as seen in Fig. 14a, and stable after repetitive cycling. In contrast, an annealed PANI electrode showed quite different characteristics (Fig. 14b). The first cycle showed an oxidation peak at 0.4 V with no cathodic counterpart. After five cycles, the redox activity of the PANI film became stable and resembled that of Fig. 14a. Thus, in a buffer solution, PANI becomes doped but requires a significant break-in procedure. Comparing the data in Fig. 14, it appears that the Pt nanoparticles present in the film maintain PANI in a redox active state. This is a significant result as it opens up the potential use of PANI/Pt composites at neutral pH without any need for pre-treatment.

Conclusions

It has been demonstrated that metallic platinum is formed in situ by the reduction of K_2PtCl_4 in PANI solutions of various solvents. The driving force for this reaction is the oxidation of PANI(EB) which reduces the PtCl_4^{2-} ions in the solution to Pt. The extent of Pt formation is highly dependent on the solvent used. In situ nanoparticle formation was least favoured in NMP and most favoured in formic acid. This is due to the aprotic nature of NMP in which the electroless process cannot be sustained by a cycle of polymer reprotonation and reduction. However, DMSO, another aprotic solvent, showed extensive in situ Pt nanoparticle formation which suggests that the redox reaction between PtCl_4^{2-} and PANI(EB) is more facile in this solvent than in NMP.

It has also been shown that spontaneous deposition of platinum particles and clusters occurs at thin films of PANI (EB) and PANI/Pt placed into solutions of K_2PtCl_4 . Thin film electrodes fabricated by this method were found to be highly electrocatalytically active for the HER, hydrazine oxidation and dichromate reduction. Formation of Pt at a PANI/Pt film resulted in the highest activity, and the surfaces of these films were found to be covered with a homogenous distribution of 1 to 2-nm-size platinum nanoparticles. The ease of fabrication of these electrodes, which are electrocatalytically active in both acidic and neutral

media, may be of interest for biosensor applications as well as in electrocatalysis as considered in this paper.

Acknowledgements We thank the EU Human Potential Programme SUSANA (Supramolecular Self-Assembly of Interfacial Nanostructures), contract HPRN-CT-2002-00185 for the funding. We are especially grateful to Steve York (Department of Physics, University of Warwick) for the TEM images.

References

- Gangopadhyay R, De A (2000) *Chem Mater* 12:608
- Schnitzler DC, Meruvia MS, Hümmelgen IA, Zarbin AJ (2003) *Chem Mater* 15:4658
- Christine M-C, Astruc D (2004) *Chem Rev* 104:293
- Qi Z, Pickup PG (1998) *Chem Commun* 21:2299
- Napporn WT, Laborde H, Léger J-M, Lamy C (1996) *J Electroanal Chem* 404:153
- Croissant MJ, Napporn T, Léger J-M, Lamy C (1998) *Electrochim Acta* 43:2447
- Sin BC, Wolf MO (2005) *Chem Comm* 3375
- Grzeszczuk M, Poks P (2000) *Electrochim Acta* 45:4171
- Castro Luna AM (2000) *J Appl Electrochem* 30:1137
- Kitani A, Akashi T, Sugimoto K, Ito S (2001) *Synth Met* 121:1301
- Kessler T, Castro Luna AM (2002) *J Appl Electrochem* 32:825
- Niu L, Li Q, Wei F, Chen X, Wang H (2003) *J Electroanal Chem* 544:121
- Niu L, Li Q, Wei F, Chen X, Wang H (2003) *Synth Met* 139:271
- Venancio EC, Napporn WT, Motheo AJ (2002) *Electrochim Acta* 47:1495
- Kim J-H, Cho J-H, Cha GS, Lee C-W, Kim H-B, Paek S-H (2000) *Biosens Bioelectron* 14:907
- Matsui J, Akamatsu K, Nishiguchi S, Miyoshi D, Nawafune DH, Tamaki HK, Sugimoto N (2004) *Anal Chem* 76:1310
- Hu C-C, Chen E, Lin J-Y (2002) *Electrochim Acta* 47:2741
- Malik MA, Galkowski MT, Bala H, Grzybowska B, Kulesza J (1999) *Electrochim Acta* 44:2157
- Breimer MA, Yevgeny G, Sheldon S, Sadik OA (2001) *Nano Lett* 1:305
- Wang J, Neoh KG, Kang ET (2001) *J Colloid Interface Sci* 239:78
- Sarma TK, Chowdhury D, Paul A, Chattopadhyay A (2002) *Chem Commun* 10:1048
- Zhou Y, Itoh H, Uemura T, Naka K, Chujo Y (2001) *Chem Commun* 7:613
- Zhou Y, Itoh H, Uemura T, Naka K, Chujo Y (2002) *Langmuir* 18:5287
- Zhai L, McCulloch RD (2004) *J Mater Chem* 14:141
- Corbierre MK, Cameron NS, Sutton M, Mochrie SG, Lurio LB, Rühm A, Lennox RB (2001) *J Am Chem Soc* 123:10411
- MacDiarmid AG, Epstein AJ (1995) *Synth Met* 69:85
- Chartier P, Mattes B, Reiss H (1992) *J Phys Chem* 96:3556
- Neoh KG, Young TT, Looi NT, Kang ET (1997) *Chem Mater* 9:2906
- Hatchett DW, Josowicz M, Janata J (1999) *Chem Mater* 11:2989
- Smith JA, Josowicz M, Janata J (2003) *J Electrochem Soc* 150: E384
- Drelinkiewicz A, Hasik M, Choczynski M (1998) *Mater Res Bull* 33:739
- Park J-E, Park S-G, Koukitu A, Hatozaki O, Oyama N (2004) *Synth Met* 141:265
- Tsakova V, Milchev A (1991) *Electrochim Acta* 36:1151

34. de Barros RA, de Azevedo WM, de Aguiar FM (2003) *Mater Charact* 50:131
35. Ivanov S, Tsakova V (2002) *J Appl Electrochem* 32:701
36. Ivanov S, Tsakova V (2002) *J Appl Electrochem* 32:709
37. Hopkins AR, Rasmussen PG, Basheer RA (1996) *Macromolecules* 29:7838
38. Mikhaylova AA, Molodkina EB, Khazova OA, Bagotzky VS (2001) *J Electroanal Chem* 509:119
39. Malinauskas A (1999) *Synth Met* 107:75
40. Gholamian M, Contractor AQ (1990) *J Electroanal Chem* 289:69
41. Nappom WT, Léger J-M, Lamy C (1996) *J Electroanal Chem* 408:141
42. Maksimov YM, Gladysheva TD, Podlovchenko BI (2001) *Russ J Electrochem* 37:653
43. Grzeszczuk M (1994) *Electrochim Acta* 39:1809
44. Grzeszczuk M, Poks P (2000) *Electrochim Acta* 45:4171
45. Lai EK, Beattie PD, Holdcroft S (1997) *Synth Met* 84:87
46. Lai EK, Beattie PD, Orfño FP, Simon E, Holdcroft S (1999) *Electrochim Acta* 44:2559
47. Coutanceau C, Croissant MJ, Napporn T, Lamy C (2000) *Electrochim Acta* 46:579
48. Cao Y, Qiu J, Smith P (1995) *Synth Met* 69:187
49. Mourata A, Viana AS, Correia JP, Siegenthaler H, Abrantes LM (2004) *Electrochim Acta* 49:2249
50. Yamada K, Yasuda K, Fujiwara N, Siroma Z, Tanaka H, Miyazaki Y, Kobayashi T (2003) *Electrochem Commun* 5:892
51. Yamada K, Asazawa K, Yasuda K, Ioroi T, Tanaka H, Miyazaki Y, Kobayashi T (2003) *J Power Sources* 115:236
52. Casella IG, Guascito MR, Salvi AM, Desimoni E (1997) *Anal Chim Acta* 354:333
53. Golabi SM, Zare HR (1999) *J Electroanal Chem* 465:168
54. Burke LD, Nugent PF (1997) *Electrochim Acta* 42:399
55. Horányi G (2000) *J Solid State Electrochem* 4:153
56. O'Mullane AP, Dale SE, Macpherson JV, Unwin PR (2004) *Chem Comm* 1606
57. Huang WS, MacDiarmid AG (1993) *Polymer* 34:1833
58. Moon D-K, Ezuka M, Maruyama T, Osakada K, Yamamoto T (1993) *Macromolecules* 26:364
59. Takanori T, Umemura J (1997) *Appl Spectrosc* 51:944
60. Chinn D, Janata J (1994) *Thin Solid Films* 252:145
61. Hasik M, Paluszkiwicz C, Wenda E (2002) *Vibr Spectrosc* 29:191
62. Fukuoka A, Sakamoto Y, Guan S, Inagaki S, Sugimoto N, Fukushima Y, Hirahara K, Iijima S, Ichikawa M (2001) *J Am Chem Soc* 123:3373
63. Fukuoka A, Higashimoto N, Sakamoto Y, Inagaki S, Fukushima Y, Ichikawa M (2001) *Microporous Mesoporous Mater* 48:171
64. Zheng W, Angelopoulos M, Epstein AJ, MacDiarmid AG (1997) *Macromolecules* 30:7634
65. Angelopoulos M, Dipietro R, Zheng WG, MacDiarmid AG (1997) *Synth Met* 84:35